

Synthesis of two quinolines from one substrate: The beginning of regulating the duality of free radicals

Runwei Jiao,^{‡a,b} Xuhong Ren,^{‡a} Xiheng Li,^{a,b} Shitao Sun,^a Hao Zhu,^a Bin Lin,^a Huiming Hua,^a Dahong Li^{*a} and Xinhua He^{*b}

a. Key Laboratory of Structure-Based Drug Design & Discovery, Ministry of Education Shenyang Pharmaceutical University; Shenyang 110016, China. E-mail: lidahong0203@163.com

b. State Key Laboratory of Toxicology and Medical Countermeasures, Beijing Institute of Pharmacology and Toxicology; Haidian district, Beijing 100850, China. E-mail: hexinhua01@126.com

[†] Electronic supplementary information (ESI) available: Experimental section and additional figures and tables. CCDC 2167675 and 2167713 (3s and 5d).

[‡] These authors contributed equally to this work.

Poly-substituted quinolines are scaffolds with diverse applications as pharmaceuticals, agrochemicals, electroluminescent materials, and dyestuffs. Herein, we present an effective scheme for the green synthesis of two multiply substituted quinoline derivatives from a singular substrate via regulating free-radical duality. Photo-catalytically generated imine radicals can undergo intramolecular Michael addition (nucleophilic 1,4-addition) to produce 3,4-disubstituted quinolines via a novel rearrangement in the presence of an inorganic base. Alternatively, they can react via an intramolecular anti-Michael addition (electrophilic 1,3-addition) in the presence of an organic base to furnish 2,3-disubstituted quinolines. The high-atom economy, good yields, mild reaction condition, simple experimental setup of this methodology, will prompt the development of Poly-substituted quinolines and other heterocycles synthesis via using intramolecular Michael addition and anti-Michael addition of free radicals. Moreover, our results suggests the theory that the electrophilic / nucleophilic bias of free radicals is determined by their structure is incomplete, the electrophilic/nucleophilic bias can be regulated by altering the reaction conditions, which can improve the efficiency of divergent synthesis.

Introduction

Quinoline is an important natural heterocycle with a structural framework which is common to various bioactive molecules^{1,2}. As shown in Fig. 1, multiply substituted quinolines serve as privileged scaffolds in many synthetic therapeutics with a wide array of physiological attributes as potential anticancer³⁻⁷, antiviral^{8,9}, antifibrotic¹⁰, antimalarial¹¹⁻¹⁴, and anti-inflammatory drugs¹⁵⁻¹⁸. Moreover, poly-substituted quinolines have unique applications as agrochemicals (pyrroloquinoline quinone)¹⁹, electroluminescent materials (8-hydroxyquinoline)²⁰⁻²², and dyestuffs (quinoline yellow)²³. To date, the methods proposed for the synthesis of multiply substituted quinolines include the [4+2] cycloaddition of aromatic imines and methyl propiolate, cyclisation of 2-aminobenzaldehyde and cyclohexane-1,3-dione, etc., or substitution reactions on existing quinoline scaffolds (Scheme 1). However, these methods have disadvantages, such as expensive and dangerous materials, non-green solvents, multi-step process, and high temperature. For example, the method of Xiaochen Ji et al uses noble metal palladium and methyl acrylate, which is toxic and stinky^{24,25}. As far as Mandeep Kaur's method is concerned, bimetallic Au-Fe₃O₄ Nano-Hybrid is expensive, and methyl propiolate is toxic, corrosive and highly irritating²⁶. CF₃-ynones is not a cheap and easily available reagent, and its preparation usually requires a complex process²⁷. The method of J. Zeng et al need to use Grignard reagent and Ti(OEt)₄, which are hazardous and moisture sensitivity²⁸. The method of Masayuki Wasa et al needs high temperature and uses noble metal Pd0 and PCy₂tBu-HBF₄, the latter is skin corrosive /irritant²⁹. Similarly, the method of Adam J. S. J. el al uses noble metal contained catalyst cataCxiium A-Pd-G3, and needs high temperature too³⁰. The methods of Pin Xu et al uses formamid and large amount of hydrochloric acid. Formamid is hygroscopic, flammable and can strongly corrode copper, brass, lead and rubber³¹. Coupling of O-Acyl Oximes with Isatins to generate quinoline-4-carboxamides needs high temperature and the use of toxic solvent toluene³². Therefore, it is essential to explore facile, effective, and green synthetic methods for these unique compounds that have several potential applications in diverse fields of interest. Herein, we present a productive scheme for the synthesis of two quinolines from a singular substrate via exploiting the duality of free radicals under the synergistic catalysis of light and non-noble metal copper salts.

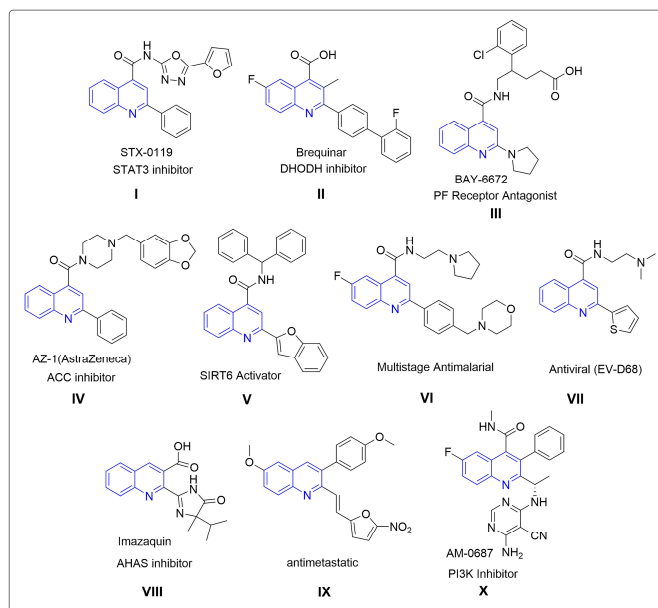
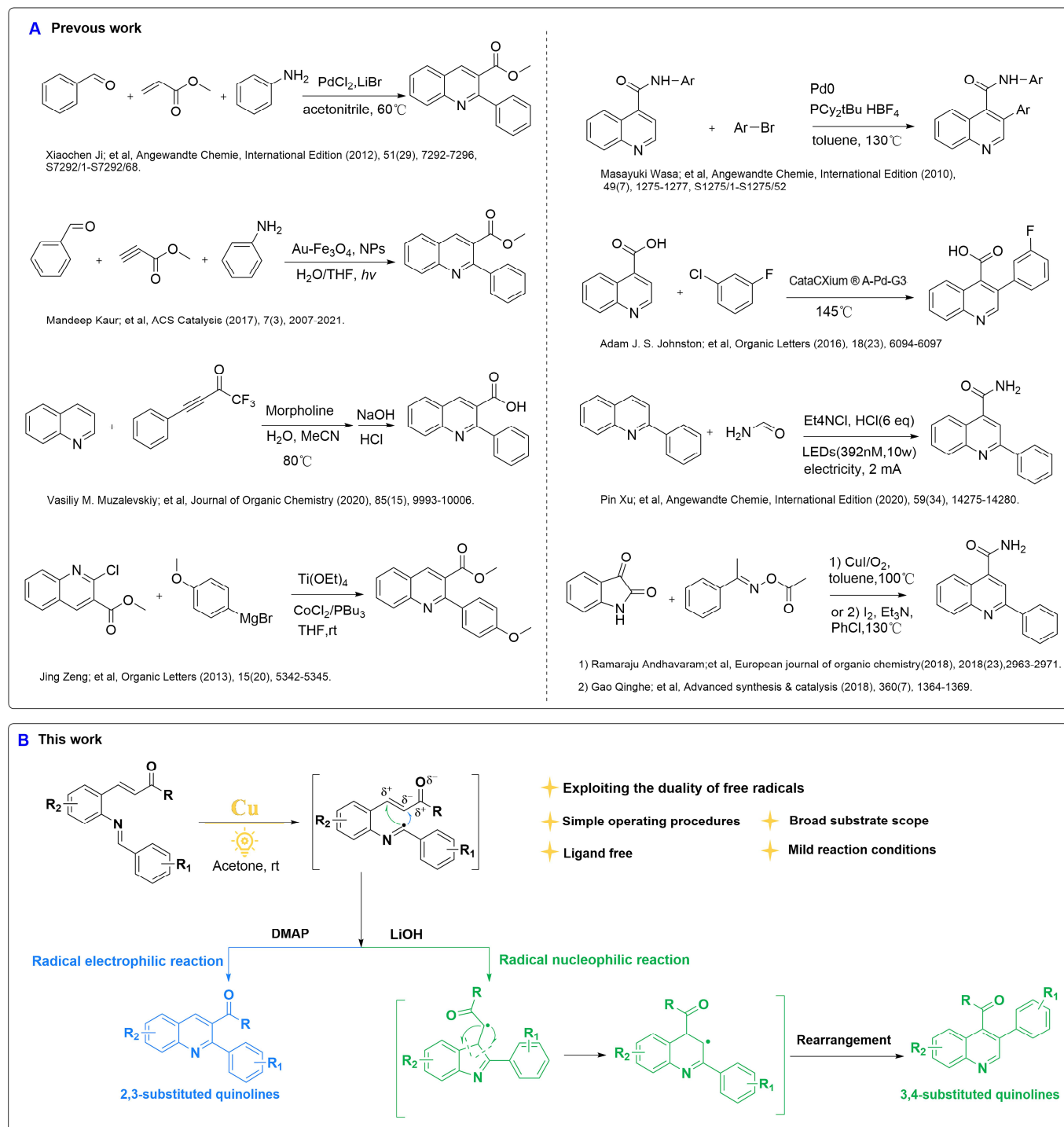


Fig. 1 Bioactive molecules of multiply substituted quinolines.

Free radicals are highly reactive species containing unpaired electrons. Their chemistry plays a key role in organic syntheses, as many transformations, which are not possible via ionic chemistry, can be readily accomplished via free-radical reactions³³⁻³⁹. However, depending on its molecular structure, a free radical can only participate in either a nucleophilic or an electrophilic reaction. Over the years, various theoretical studies have been attempted to characterise the properties of free radicals and predict their electrophilic–nucleophilic bias in chemical reactions⁴⁰⁻⁴². For example, Pérez et al. have introduced a set of density functional theory (DFT) reactivity indices to determine the electrophilicity or nucleophilicity of a free radical^{43, 44}.

According to this theory, free radicals can participate in diverse reactions, contributing significantly to the construction of chemical bonds such as C-C, C-N, C-B, C-O, and C-F⁴⁵⁻⁴⁸. There are many examples of free-radical reactions that are nucleophilic in nature. As an example, Leonori et al. fabricated C-C bonds in a wide range of redox conversions involving aminoalkyl radicals, aryl halides, and borated azines using an ammoniacal borane reagent via photocatalysis^{49, 50}; Xu et al. devised the cyclisation of free radicals via electrocatalysis to form key C-N bonds; and Patel et al. difunctionalised alkynes to C-O and C-S linkages under mediation by visible light^{51, 52}. Similarly, examples of free-radical electrophilic reactions are relatively common. Notable efforts include dual copper–photo-redox catalysis to achieve trifluoromethylation of aryl bromides by MacMillan and co-workers, the development of a photolytic method for direct benzyl fluorination using cheap and readily available diarylketones as catalysts by Chen et al.^{53, 54}, a photochemical, three-component Minisci reaction by coupling 1,3-dicarbonyl compounds as reported by Xia et al., and the fabrication of C-N bonds by employing the ability of nitrogen radicals to undergo strain-release reactions with [1.1.1]Propellane as reported by Leonori et al.^{55, 56}. In addition, Palacios et al. have studied the photo-stimulated reactions between haloarenes and potassium diphenylarsenide in liquid ammonia to successfully synthesise the C-As bond. In another study, Lu et al. have fabricated C-O, C-Br, C-I, C-C, and C-N bonds with high selectivity using a copper catalyst at elevated temperatures^{57, 58}. Thus, it is well established, theoretically and practically, that the electrophilic–nucleophilic bias of free radicals depends on their structure and that free radicals are either electrophilic or nucleophilic during organic reactions. Therefore, it is natural to explore if this bias can be regulated by changing the reaction conditions. If this regulation is achieved, the opportunity for free radicals to undergo novel reactions can be doubly enhanced. To achieve this objective, we envisioned the development of distinct synthetic protocols to regulate the electrophilic–nucleophilic bias of free radicals for the synthesis of multiply substituted quinolines in a productive fashion. Further, we wanted to extend the addition reactions of α , β -unsaturated ketones, namely Michael addition and anti-Michael addition⁵⁹⁻⁶¹, to involve free radicals as substrates. In this regard, the imine C-H bond of (*E*)-3-(2-(((*E*)-benzylidene)amino)phenyl)acrylate was photoactivated to obtain the imine carbon radical. The addition of *N,N*-dimethylpyridin-4-amine (DMAP) facilitated the electrophilic attack of the imine carbon free radical on the α position of the

acrylate to form 2,3-disubstituted quinolines via intramolecular cyclisation. In contrast, the addition of lithium hydroxide (LiOH) facilitated the nucleophilic attack of the imine carbon free radical on the β position of the acrylate to form 3,4-disubstituted quinolines via a complicated rearrangement. These methods for the synthesis of poly-substituted quinolines exhibit various advantages, such as, mild reaction conditions, facile and simple setup and operation, biodegradability, and a good functional group tolerance. The reaction mechanisms explored in this study are proposed based on theoretical calculations and experimental observations. The examples discussed in this work demonstrate the possibility of regulating the electrophilicity and nucleophilicity of free radicals via changes in the reaction conditions and suggest novel opportunities for free-radical addition reactions.



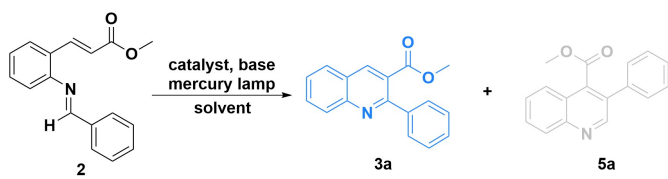
Scheme 1 Exploiting the duality of free radicals for the productive synthesis of two quinolines from one substrate.

Results and discussion

Reaction discovery and optimisation. To determine whether the nucleophilicity and electrophilicity of free radicals could be regulated and utilised for the efficient synthesis of various compounds from the same precursor, we studied the intramolecular Michael addition and anti-Michael addition reactions of methyl (*E*)-3-(2-(((*E*)-benzylidene)amino)phenyl)acrylate (**2**). In our previous work, we had reported that an imine C-H bond can be photoactivated to generate a carbon radical⁶². Theoretically, if the nucleophilicity and electrophilicity of free radicals could be regulated by altering the reaction conditions, the resulting carbon radical could be programmed to attack either the α or β position in **2** to form methyl 2-phenylquinoline-3-carboxylate (**3a**) or methyl 2-(2-phenyl-3*H*-indol-3-ylidene)acetate (**4a**), respectively. To evaluate this hypothesis, various reaction conditions were investigated and indeed, the synthesis of **3a** was successfully achieved. However, even after numerous attempts, **4a** could not be synthesised. Further investigations suggested that **4a** rearranged to form methyl 3-phenylquinoline-4-carboxylate (**5a**), as shown in Scheme 1. Based on these observations, the reaction conditions were subsequently optimised to regulate the nucleophilicity and electrophilicity of the imine carbon radical to improve the yield of both **3a** and **5a** entities.

To optimise the synthesis of **3a**, a plethora of reaction conditions, including the catalysts, solvents, bases, temperature, humidity, and molar ratios, were extensively explored. Firstly, the effect of the catalyst, CoCl₂, was investigated using Cs₂CO₃ as the base and acetone as the solvent (Table 1, entry 1), and both **3a** and **5a** were obtained in low yield. Next, CoCl₂ was replaced with various catalysts, namely, FeCl₃, Cu(CF₃COO)₂, Co(OAc)₂, and CuO to ascertain the effect of the catalyst on product formation. Among these, Cu(CF₃COO)₂ emerged as the catalyst of choice, affording **3a** in good yield within a reaction time of 4 h. Next, with Cu(CF₃COO)₂ as the optimal catalyst, the reaction media was varied and six distinct solvents, namely acetone, ethanol, THF, DMF, IPA, and EA, were assessed to ascertain product formation (Table 1, entries 6–11). The results clearly indicate that using acetone as the reaction solvent led to the highest yield (67%) of **3a** (Table 1, entry 6) which further increased to 96% when the base was changed to DMAP. This particular reaction was also catalysed by 5 mol% Cu(CF₃COO)₂ and facilitated using mercury lamp irradiation (Table 1, entry 20).

Table 1 Reaction optimization and control experiments for **3a**.^[a]



Entry	Solvent	Base	Catalyst	Time (h)	3a Yield ^[b] (%)	5a (%)
1	Acetone	Cs ₂ CO ₃	CoCl ₂	3	11	7
2	DMF	Cs ₂ CO ₃	CoCl ₂	3	2	-
3	Acetone	DBU	Co(OAc) ₂	8	57	-
4	Acetone	Cs ₂ CO ₃	FeCl ₃	3.5	50	-
5	Acetone	Cs ₂ CO ₃	CuO	8	59	-
6	Acetone	Cs ₂ CO ₃	Cu(CF ₃ COO) ₂	4	67	-
7	Ethanol	Cs ₂ CO ₃	Cu(CF ₃ COO) ₂	9	25	-
8	THF ^[c]	Cs ₂ CO ₃	Cu(CF ₃ COO) ₂	5	4	5
9	DMF ^[d]	Cs ₂ CO ₃	Cu(CF ₃ COO) ₂	4	-	-
10	EA ^[e]	Cs ₂ CO ₃	Cu(CF ₃ COO) ₂	11	46	-
11	IPA ^[f]	Cs ₂ CO ₃	Cu(CF ₃ COO) ₂	22	55	-
12	Ethanol	DMAP ^[g]	Cu(CF ₃ COO) ₂	5	62	-
13	Acetone	K ₂ CO ₃	Cu(CF ₃ COO) ₂	9	63	-
14	Acetone	CsOAc	Cu(CF ₃ COO) ₂	4	58	-
15	Acetone	NMM ^[h]	CuOAc	7	11	-
16	Acetone	DIPEA ^[i]	CuBr ₂	8	34	-
17	Acetone	Pyridine	Cu(CF ₃ COO) ₂	5	45	-
18	Acetone	HOBT ^[j]	Cu(CF ₃ COO) ₂	3	19	11
19	Acetone	-	Cu(OH) ₂	4	39	-
20	Acetone	DMAP	Cu(CF ₃ COO) ₂	3	96(85) ^[k]	-
21	Acetone	DMAP	Cu(CF ₃ COO) ₂ , no light	24	-	-
22	Acetone	DMAP	Cu(CF ₃ COO) ₂ , N ₂	24	-	-
23	Acetone	DMAP	3% Cu(CF ₃ COO) ₂	3	81	-
24	Acetone	DMAP	1% Cu(CF ₃ COO) ₂	3	43	-

[a] Unless otherwise specified, the reaction of **2** (1 mmol), catalyst (5 mol%), and base (1 mmol) was carried out in 250 mL of solvent. [b] HPLC yields. [c] THF, tetrahydrofuran. [d] DMF, dimethyl formamide. [e] EA, ethyl acetate. [f] IPA, isopropanol. [g] DMAP, 4-dimethylaminopyridine. [h] NMM, 4-methylmorpholine. [i] DIPEA, *N,N*-diisopropylethylamine. [j] HOBT, 1-hydroxybenzotriazole. [k] Isolated yield.

We also examined if Cs_2CO_3 could be replaced by other bases to improve the yield of **5a**. As shown in Table 2, LiOH was found to be the most suitable among the inorganic bases that were screened (entries 3–7). Further optimisation revealed that product **5a** was formed in 60% yield using a combination of 0.5 equiv. of LiOH and 20 mol% of $\text{Cu}(\text{CF}_3\text{COO})_2$ (Table 2, entry 13). Finally, several control experiments were performed to address the role of the bases, the metal catalysts, and the presence/absence or nature of irradiation. Only trace amounts of **3a** and **5a** were obtained in the absence of light, a base, or $\text{Cu}(\text{CF}_3\text{COO})_2$ (Table 2, entries 8 and 14–16) which clearly indicated that a photo-redox catalytic system was essential for the transformation. Notably, the reaction was observed to be critically dependent on the presence of molecular oxygen. For instance, when the reactions were conducted in a nitrogen atmosphere, no product was formed, and the substrate (**2**) remained unchanged (Table 2, entry 17). Moreover, assuming a dual free-radical mechanism for the reaction, the low yield could be explained by the generation of fewer or less reactive free radicals by the substrate. Various other additives, such as, nitrene, azo, peroxide, and some metal salts were also tested together with a change in the wavelength of irradiation (400–780 nm) to influence product yield. However, none of these factors led to any desired increase in the yield of **3a** and **5a**, and in most cases, no product formation was achieved (see Supplementary Information section 3.5.3).

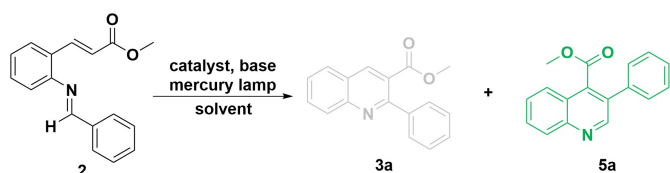


Table 2 Reaction optimization and control experiments for **5a**.^[a]

Entry	Solvent	Base	Catalyst	Time (h)	3a Yield ^[b] (%)	5a (%)
1	Acetone	NaOH ^[c]	5% $\text{Cu}(\text{CF}_3\text{COO})_2$	1.5	5	18
2	Acetone	NaOH	10% $\text{Cu}(\text{CF}_3\text{COO})_2$	1.5	16	47
3	Acetone	NaOH	20% $\text{Cu}(\text{CF}_3\text{COO})_2$	1.5	15	55
4	Acetone	LiOH ^[d]	20% $\text{Cu}(\text{CF}_3\text{COO})_2$	1.4	14	58
5	Acetone	KOH ^[e]	20% $\text{Cu}(\text{CF}_3\text{COO})_2$	1.4	11	47
6	Acetone	RbOH ^[f]	20% $\text{Cu}(\text{CF}_3\text{COO})_2$	1.5	12	43
7	Acetone	CsOH ^[g]	20% $\text{Cu}(\text{CF}_3\text{COO})_2$	1.5	39	23
8	Acetone	-	20% $\text{Cu}(\text{CF}_3\text{COO})_2$	2.0	14	15
9	Ethanol	LiOH	20% $\text{Cu}(\text{CF}_3\text{COO})_2$	12.0	24	-
10	THF ^g	LiOH	20% $\text{Cu}(\text{CF}_3\text{COO})_2$	8.0	2	-
11	Acetone	LiOH	20% CuO	4.0	18	-
12	Acetone	LiOH	20% CoCl_2	5.0	3	4
13	Acetone	0.5 eq. LiOH	20% $\text{Cu}(\text{CF}_3\text{COO})_2$	1.3	16	60(49)^h
14	Acetone	-	-	8.0	7	-
15	Acetone	0.5 eq. LiOH	-	1.0	5	-
16	Acetone	0.5 eq. LiOH	20% $\text{Cu}(\text{CF}_3\text{COO})_2$, no light	24	-	-
17	Acetone	0.5 eq. LiOH	20% $\text{Cu}(\text{CF}_3\text{COO})_2$, N₂	24	-	-

[a] Unless otherwise specified, the reaction of **2** (1 mmol), catalyst, and base (1 mmol) was carried out in 250 mL of solvent. [b] HPLC yields. [c] NaOH, sodium hydroxide. [d] LiOH, lithium hydroxide. [e] KOH, potassium hydroxide. [f] RbOH, rubidium hydroxide. [g] CsOH, caesium hydroxide. [h] Isolated yield.

Substrate scope studies. The substrate scope for the reaction is shown in Fig. 2. All substrates underwent facile free-radical electrophilic or nucleophilic reactions and furnished the corresponding products in good to excellent yield, irrespective of the presence of electron-donating or electron-withdrawing substituents on the aromatic ring. However, the electron-deficient aromatic rings were conducive to the formation of 2,3-disubstituted quinolines, whereas 3,4-disubstituted quinolines were more readily formed in the presence of electron-donating groups on the aromatic ring (**3c**, **3g**, **5b**, and **5d**) which is consistent with the electrophilic and nucleophilic free-radical reaction mechanisms, respectively. Moreover, the synthesis of 2,3-disubstituted-quinolines were tolerated by a wide range of functional groups, including the alkoxy and aryl halide groups. In fact, the comparatively unstable hydroxyl products, such as **3b** and **3k**, also remained intact during the course of the reaction, indicating the relatively mild conditions used for this method. Interestingly, the reaction conditions were also suitable for heteroarenes (**3u**, 65% yield; **5k**, 54% yield). Likewise, 3,4-disubstituted quinolines with phenyl, halo, or methoxy substituents were also

obtained in good to excellent yield. We examined the generality of the reaction conditions by replacing the ester group with amides and noted that the yield of the former derivative was mostly higher than that of the latter. Notably, both 2,3-disubstituted and 3,4-disubstituted quinolines, such as **3d**, **5d**, **5f**, and **5g**, were synthesised in the presence of methoxy groups on the peripheral aromatic ring. The structure of poly-substituted quinoline derivatives, such as **3s** and **5d**, were explicitly determined using single-crystal X-ray analysis (see Supplementary Information Figs. S1-S2) to confirm the formation of the quinoline ring and further demonstrate the effectiveness of this method for the synthesis of poly-substituted quinolines with a wide array of accompanying structural features and functional groups.

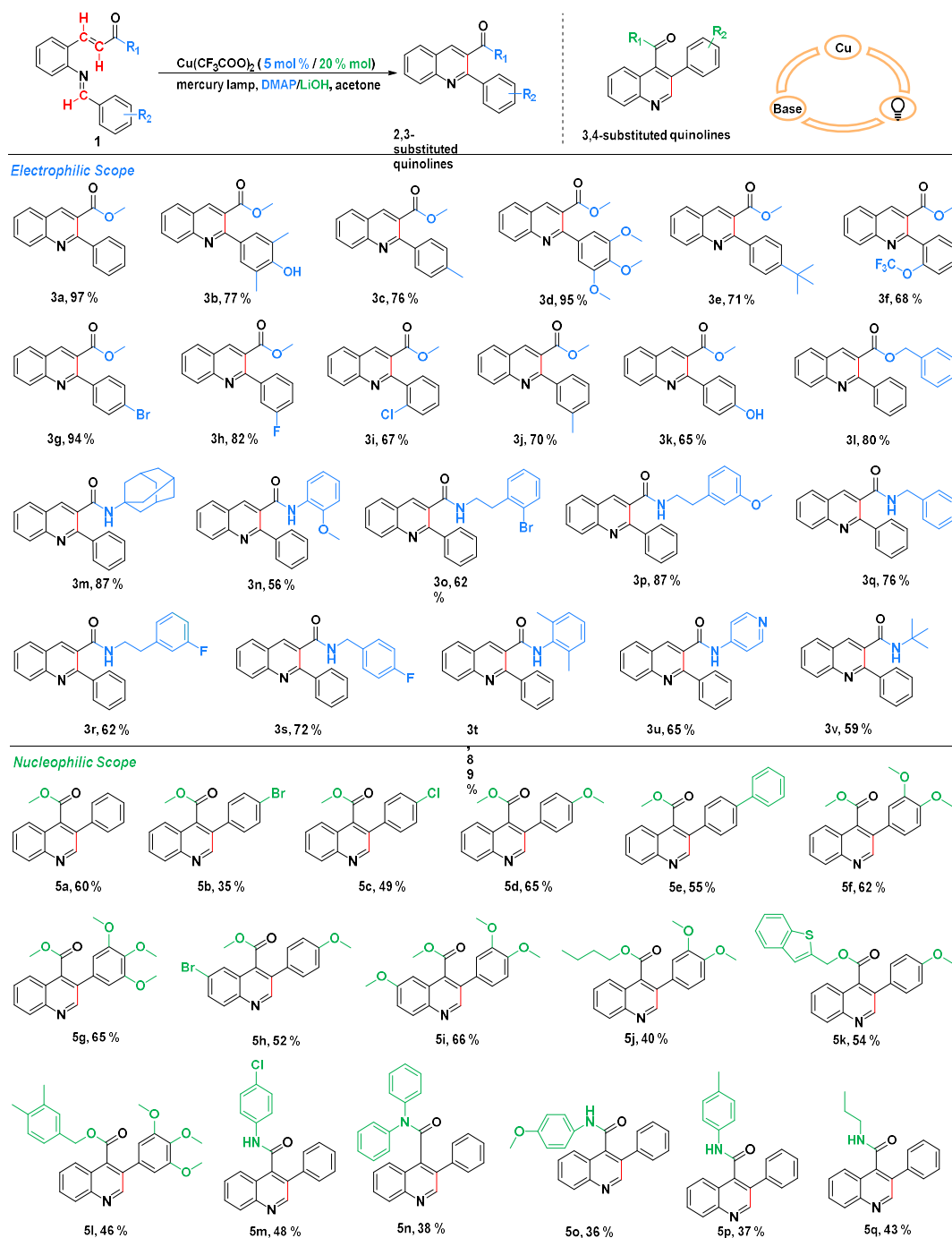


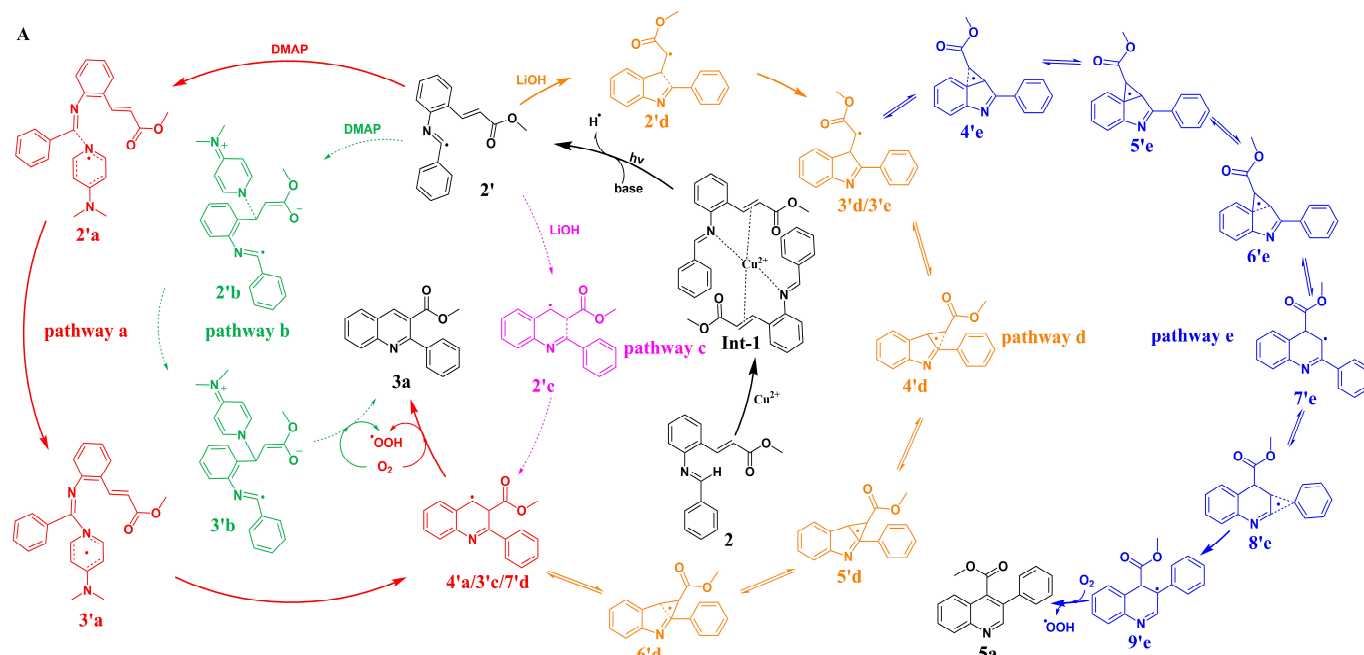
Fig. 2 Substrate scope of photocatalytic radical electrophilic and nucleophilic C-C bond construction. Electrophilic reaction conditions: substrate (1 mmol), $\text{Cu}(\text{CF}_3\text{COO})_2$ (5 mol %), DMAP (100 mol %), and acetone (250 mL), irradiation using mercury lamp at 20 - 25 °C for 2 h. Nucleophilic reaction conditions: substrate (1 mmol), $\text{Cu}(\text{CF}_3\text{COO})_2$ (20 mol %), LiOH (50 mol %), and acetone (250 mL), irradiation using

mercury lamp at RT for 1.2 h. Isolated yields after flash chromatography. The solvent can be recovered for continued use as the reaction media.

Mechanistic studies. We theorised that the imine C-H bond generates carbon radicals via photoinduction and strong base catalysis, which attack the α and β positions of the acrylate (**2**) to form products **3a** and **5a** via five possible pathways (Fig. 3A).

The reaction is initiated by the complexation of Cu(II) with the imine group and the alkene of substrate **2**^{25, 63}, forming **Int-1** (**intermediate-1**). In the next step, the complex is photoactivated to form the imine free-radical intermediate **2'**. When DMAP is used as the base, two reaction pathways, a and b, are deemed possible. In pathway **a**, the imine carbon free radical in **2'** can bind with DMAP to produce the intermediate **3'a** which can cyclise to form the intermediate **4'a**. This in turn can undergo oxidative dehydrogenation to produce **3a**. Alternatively, in pathway **b**, DMAP would initially react with the carbon atom at the β position of the α,β -unsaturated ketone to afford the intermediate **3'b** which can react with the oxygen in the vicinity to form **3a**. On the other hand, when LiOH is used as the base, there are three pathways **c**, **d**, and **e** which could be followed to yield the final product. In pathway **c**, the intermediate **2'** can cyclise to yield **2'c**, a six-membered ring, which undergoes oxidation in the last step to form **3a**. In pathway **d**, intermediate **2'** can undergo cyclisation to form the five-membered ring **3'd/3'e** which can then lead to two separate pathways **d** or **e**. In pathway **d**, **3'd/3'e** is rearranged to form **4'd** which can form the tautomers, **5'd** and **6'd**. As shown in Fig. 3A, in a penultimate step, **6'd** can undergo rearrangement to yield **4'a/3'c/7'd** which can be oxidised in the final step to form **3a**. Alternately, in pathway **e**, the **3'd/3'e** entity can also be rearranged to form **4'e** which can subsequently undergo tautomerisation to yield the intermediates **5'e**, **6'e**, and **7'e**. The **7'e** tautomer can lead to the formation of the cyclic intermediate **8'e** which can rearrange to yield **9'e**. Eventually, **9'e** can be oxidised to **5a**.

To explore the feasibility of the reaction pathways, DFT calculations were conducted using the Gaussian 09 package. The DFT method of the B3LYP functional was used with a 6-31+G(d,p) basis set to optimise the geometry of molecules in acetone. Frequency analyses were performed to verify the absence of imaginary frequencies. The solvent effect was taken into consideration with a SMD continuum solvation model⁶⁴⁻⁶⁶. The free-energy profiles of these pathways were calculated using the B3LYP method in acetone. As shown in Fig. 3B, **3a** could be theoretically obtained from intermediate **2'** via either of the two pathways, **a** or **b**. However, the free energy of the transition states for **2'a** in pathway **a** and **2'b** in pathway **b** were calculated to be 11.1 and 26.2 kcal/mol, respectively. These values clearly suggest that for the formation of **3a**, owing to its lower free energy of the transition state, pathway **a** is preferred over pathway **b**. Simultaneously, when LiOH is employed as the base, the free energy of the transition states for **2'c** in pathway **c** and **2'd** in pathway **d** were calculated as 6.2 and -2.8 kcal/mol, respectively. These results clearly indicative of the preference for pathway **d** over pathway **c** for the formation of **3a**.



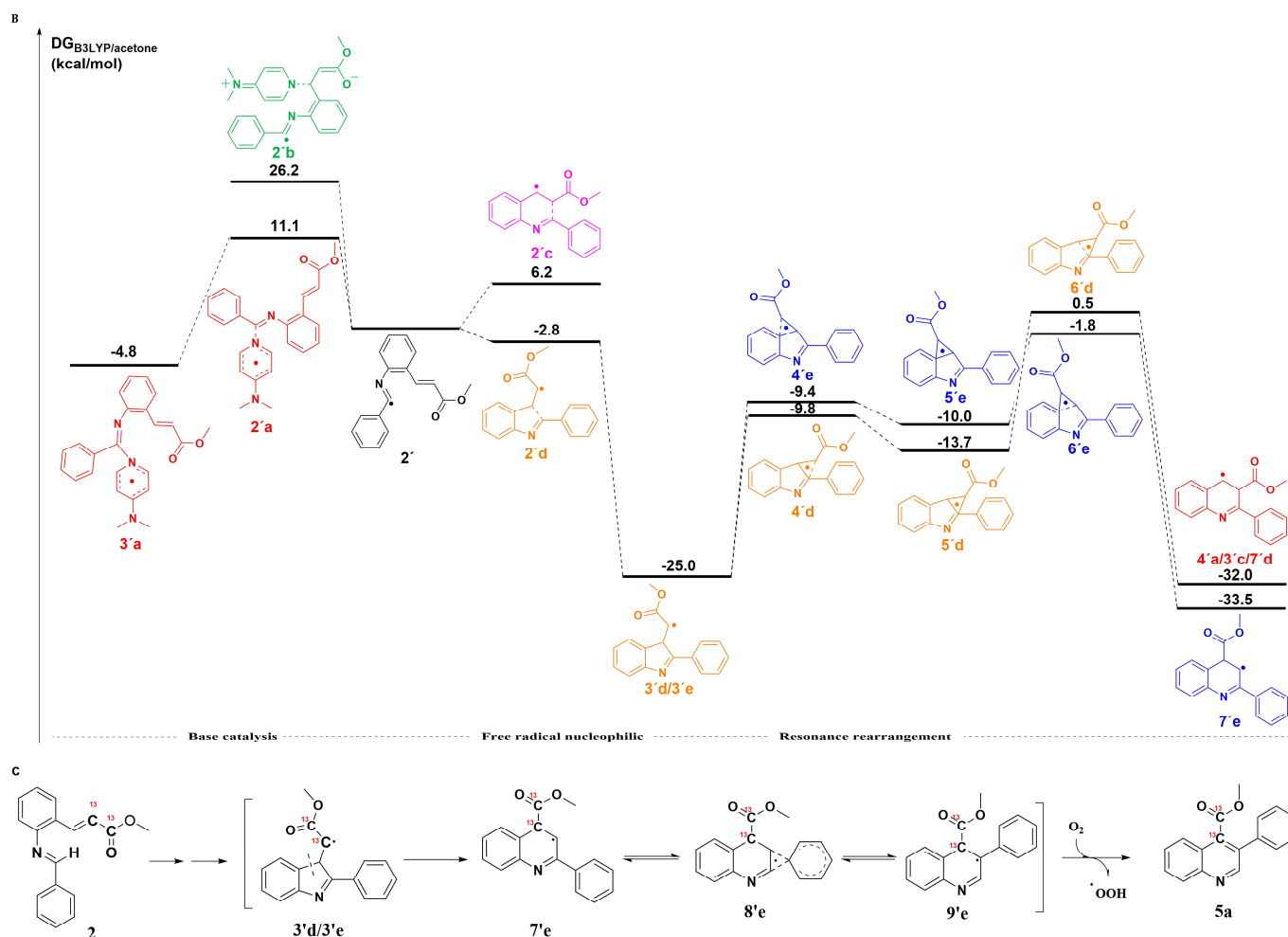


Fig. 3 (A) The proposed mechanisms for the controlled cyclisation reactions catalysed by DMAP and LiOH; (B) Free-energy profiles for pathways **a–e** (depicted in red, green, magenta, orange, and blue, corresponding to those in Fig. 3A). (C) The ^{13}C isotopic labeling experiment confirms the proposed rearrangement mechanism.

Pathways **d** and **e** share a common intermediate **3'd/3'e**. When the intermediate **3'd/3'e** undergoes rearrangement via pathway **d** to produce the intermediate **7'd**, the free energy of the transition states are calculated to be -9.8 , -13.7 , and 0.5 kcal/mol for **4'd**, **5'd**, and **6'd**, respectively. However, when the intermediate **3'd/3'e** produces **7'e** via pathway **e**, the free energy of the transition states were calculated as -9.4 , -10.0 , and -1.8 kcal/mol for **4'e**, **5'e**, and **6'e**, respectively which are slightly lower than those obtained for pathway **d**. These results suggest that in the presence of LiOH, the corresponding mechanism for the primary and secondary reactions followed pathways **e** and **d**, respectively. These results are also consistent with the experimental data, suggesting that **5a** and **3a** are the major and minor products, respectively, for the current reaction sequence. These observations further provide crucial insights into the possible mechanism of the cyclisation and rearrangement reactions, explored in this study.

A series of experiments were further conducted to verify the proposed mechanisms. To confirm the formation of the complex (**Int-1**) between **2** and Cu(II) in the solution phase, the ultraviolet–visible (UV–vis) absorption spectrum was recorded, as described in our previous study. As shown in Fig. S3, the absorption peaks observed at approximately 206, 270, and 324 nm could not be accounted for individual contributions from the spectra of substrate **2** and $Cu(CF_3COO)_2$, suggesting an association between these two species. To further investigate its structure, 1H nuclear magnetic resonance (NMR) spectra were recorded (see Supplementary Information Fig. S4) which indicate a molar ratio of 1:2 for Cu(II) and **2**. This molar ratio is also evident from the splitting pattern of the peaks in the NMR spectra for **Int-1**. The overall changes in the NMR spectra and the increase in the number of peaks also indicate that the structure of **Int-1** is composed of two molecules

of **2** and a singular copper ion. Based on these results, the UV–vis absorption spectra of the two reaction systems were further explored. The peaks observed at approximately 205, 259, 273, and 350 nm could not be accounted for by adding the contributions from the individual spectra for substrate **2**, $\text{Cu}(\text{CF}_3\text{COO})_2$, and DMAP which suggests the presence of strong interaction between **Int-1** and DMAP. However, the UV–vis absorption spectra indicate a weak interaction between **Int-1** and LiOH, and an auxiliary role of the trifluoroacetate ion (see Supplementary Information Figs. S5–S6). X-ray photoelectron spectroscopy (XPS) experiments demonstrate the presence of Cu(II) and Cu(I) ions, indicating that there are indeed Cu(I) and Cu(II) cycles that occur during the photocatalytic reaction (see Supplementary Information Fig. S7).

To confirm that the reaction proceeded via a free-radical mechanism, the radical scavenger 5-dimethyl-1-pyrroline *N*-oxide (DMPO) was used to inhibit the reactions. The addition of DMPO to a reaction mixture containing **2**, $\text{Cu}(\text{CF}_3\text{COO})_2$, and DMAP, leads to a significant decrease in the isolated yield of **3a**. In the presence or absence of DMPO, the yields of **3a** were 17% and 85%, respectively. Similarly, on using DMPO and switching the catalytic base from DMAP to LiOH, the product **5a** was not obtained, indicating that a free-radical mechanism is involved. Next, electron paramagnetic resonance (EPR) studies were performed to study the signal for free radicals. Under light irradiation, a solution of **2** did not generate any signal to indicate the presence of a free radical species. On the addition of $\text{Cu}(\text{CF}_3\text{COO})_2$ and LiOH, and subsequent reaction progress, the EPR signal indicating the presence of free radical species significantly increased. Large amounts of free radicals, including peroxide, carbon, and trifluoroacetate radicals, were generated in a solution of **2**, $\text{Cu}(\text{CF}_3\text{COO})_2$, and LiOH (see Supplementary Information Fig. S10). Under light irradiation, only a few peroxide-based free radicals were generated in a solution of **2**, $\text{Cu}(\text{CF}_3\text{COO})_2$, and DMAP which was consistent with the results of the hydrogen peroxide test (see Supplementary Information Figs. S11–S12). These results further confirmed that a free-radical mechanism was followed for the reactions discussed in this study, and copper ions and organic/inorganic bases played an important role in determining the reaction progress and subsequent product formation.

As discussed, the conversion of **2** to **5a** involves a complex rearrangement reaction, and we were curious to determine if the reaction is influenced by a temperature change. To explore this possibility, reactions were conducted across a temperature range of -10 to 25 °C using $\text{Cu}(\text{CF}_3\text{COO})_2$ as the catalyst and LiOH as the base. The ideal temperature range was found to be within $17 - 18$ °C. A study of the reaction kinetics at this temperature revealed that the yield peaked at 1.5 h and subsequently decreased, owing to the degradation of the product (see Supplementary Information Fig. S13). Finally, to study the molecular rearrangement mechanism involved in the formation of **5a**, the ester carbonyl carbon atom in molecule **2** and its α -carbon atom were labelled with isotope ^{13}C . Using the optimised reaction conditions described in this work, we obtained ^{13}C -labelled **5a** which was subsequently analysed via NMR (see Supplementary Information Figs. S14–S16). The mechanism for molecular rearrangement to produce **5a**, based on NMR analysis, is shown in Fig. 3C.

Conclusions

Poly-substituted quinolines represent an important structural motif in numerous biologically active products. Their preparation methods usually have disadvantages including expensive and dangerous materials, non-green solvents, multi-step process, and high temperature. Therefore, an efficient, green synthetic protocol for the design of multiply substituted quinoline derivatives with a wide variety of appended functional groups has tremendous practical significance. In this study, we provide a myriad of examples of photo-catalytically generated imine radicals that can undergo intramolecular electrophilic and nucleophilic addition reactions in the presence of organic and inorganic bases, respectively, to produce various poly-substituted quinoline derivatives. The high-atom economy, good yields, mild reaction condition, simple experimental setup of this methodology, will prompted the development of new protocols for other heterocycles synthesis via using intramolecular Michael addition and anti-Michael addition of free radicals. Moreover, this study also proves that the previously universally accepted theory that the electrophilic nucleophilic duality of free radicals is only determined by their structure is incomplete, and provides compelling evidence to support the hypothesis that regulating the electrophilicity and nucleophilicity of free radicals by changing the reaction conditions can facilitate the synthesis of multiple products from the same precursor material, which means that the atomic economy can be improved when synthesizing products with diverse structures.

Author Contributions

X. He conceived the idea for this work. R. Jiao, X. Ren, X. Li and H. Zhu carried out the experiments. B. Lin and S. Sun calculated the experimental results by density functional theory. X. He, D. Li and H. Hua provided guidance for the experiment. R. Jiao wrote the manuscript and revised it by X. He and D. Li.

Conflicts of interest

There are no conflicts to declare.

Acknowledgements

We thank the Beijing Institute of Technology, Shanghai Jiao Tong University, Chinainstru & Quantumtech (Hefei) Co.,Ltd. and Dalian University of Technology, where the X-ray diffraction of single crystal, EPR, and XPS analyses were performed.

Notes and references

1. T. Iwai and M. Sawamura, *ACS Catalysis*, 2015, **5**, 5031-5040.
2. Z. Guo, C. Yan and W. H. Zhu, *Angew Chem Int Ed Engl*, 2020, **59**, 9812-9825.
3. J. T. Madak, C. R. Cuthbertson, Y. Miyata, S. Tamura, E. M. Petrunak, J. A. Stuckey, Y. Han, M. He, D. Sun, H. D. Showalter and N. Neamati, *J Med Chem*, 2018, **61**, 5162-5186.
4. X. Chen, W. Sun, S. Huang, H. Zhang, G. Lin, H. Li, J. Qiao, L. Li and S. Yang, *J Med Chem*, 2020, **63**, 10474-10495.
5. H. Li, Q. Yao, F. Xu, Y. Li, D. Kim, J. Chung, G. Baek, X. Wu, P. F. Hillman, E. Y. Lee, H. Ge, J. Fan, J. Wang, S. J. Nam, X. Peng and J. Yoon, *Angew Chem Int Ed Engl*, 2020, **59**, 10186-10195.
6. O. Afzal, S. Kumar, M. R. Haider, M. R. Ali, R. Kumar, M. Jaggi and S. Bawa, *Eur J Med Chem*, 2015, **97**, 871-910.
7. Y. S. Haojie Jin, Yuanyuan Lv, Shengxian Yuan, Christel F. A. Ramirez, Cor Lieftink, Liqin Wang, Siying Wang, Cun Wang, Matheus Henrique Dias, Fleur Jochems, Yuan Yang, Astrid Bosma, E. Marielle Hijmans, Marnix H. P. de Groot, Serena Vegna, Dan Cui, Yangyang Zhou, Jing Ling, Hui Wang, Yuchen Guo, Xingling Zheng, Nikita Isima, Haiqiu Wu, Chong Sun, Roderick L. Beijersbergen, Leila Akkari, Weiping Zhou, Bo Zhai, Wenxin Qin, René Bernards, *Nature*, 2021, **595**, 730-734.
8. R. Musharrafieh, J. Zhang, P. Tuohy, N. Kitamura, S. S. Bellampalli, Y. Hu, R. Khanna and J. Wang, *J Med Chem*, 2019, **62**, 4074-4090.
9. R. Kaur and K. Kumar, *Eur J Med Chem*, 2021, **215**, 113220.
10. K. Jansen, L. Heirbaut, R. Verkerk, J. D. Cheng, J. Joossens, P. Cos, L. Maes, A. M. Lambeir, I. De Meester, K. Augustyns and P. Van der Veken, *J Med Chem*, 2014, **57**, 3053-3074.
11. Y. Zhang, J. A. Clark, M. C. Connelly, F. Zhu, J. Min, W. A. Guiguemde, A. Pradhan, L. Iyer, A. Furimsky, J. Gow, T. Parman, F. El Mazouni, M. A. Phillips, D. E. Kyle, J. Mirsalis and R. K. Guy, *J Med Chem*, 2012, **55**, 4205-4219.
12. P. M. O'Neill and S. A. Ward, *Angew Chem Int Ed Engl*, 2015, **54**, 13504-13506.
13. Y. Q. Hu, C. Gao, S. Zhang, L. Xu, Z. Xu, L. S. Feng, X. Wu and F. Zhao, *Eur J Med Chem*, 2017, **139**, 22-47.
14. B. Baragana, I. Hallyburton, M. C. Lee, N. R. Norcross, R. Grimaldi, T. D. Otto, W. R. Proto, A. M. Blagborough, S. Meister, G. Wirjanata, A. Ruecker, L. M. Upton, T. S. Abraham, M. J. Almeida, A. Pradhan, A. Porzelle, T. Luksch, M. S. Martinez, T. Luksch, J. M. Bolscher, A. Woodland, S. Norval, F. Zuccotto, J. Thomas, F. Simeons, L. Stojanovski, M. Osuna-Cabello, P. M. Brock, T. S. Churcher, K. A. Sala, S. E. Zakutansky, M. B. Jimenez-Diaz, L. M. Sanz, J. Riley, R. Basak, M. Campbell, V. M. Avery, R. W. Sauerwein, K. J. Dechering, R. Noviyanti, B. Campo, J. A. Frearson, I. Angulo-Barturen, S. Ferrer-Bazaga, F. J. Gamo, P. G. Wyatt, D. Leroy, P. Siegl, M. J. Delves, D. E. Kyle, S. Wittlin, J. Marfurt, R. N. Price, R. E. Sinden, E. A. Winzeler, S. A. Charman, L. Bebrevska, D. W. Gray, S. Campbell, A. H. Fairlamb, P. A. Willis, J. C. Rayner, D. A. Fidock, K. D. Read and I. H. Gilbert, *Nature*, 2015, **522**, 315-320.

15. T. D. Cushing, X. Hao, Y. Shin, K. Andrews, M. Brown, M. Cardozo, Y. Chen, J. Duquette, B. Fisher, F. Gonzalez-Lopez de Turiso, X. He, K. R. Henne, Y. L. Hu, R. Hungate, M. G. Johnson, R. C. Kelly, B. Lucas, J. D. McCarter, L. R. McGee, J. C. Medina, T. San Miguel, D. Mohn, V. Pattaropong, L. H. Pettus, A. Reichelt, R. M. Rzasa, J. Seganish, A. S. Tasker, R. C. Wahl, S. Wannberg, D. A. Whittington, J. Whoriskey, G. Yu, L. Zalameda, D. Zhang and D. P. Metz, *J Med Chem*, 2015, **58**, 480-511.
16. M. H. Abdelrahman, B. G. M. Youssif, M. A. Abdelgawad, A. H. Abdelazeem, H. M. Ibrahim, A. Moustafa, L. Treاملu and S. N. A. Bukhari, *Eur J Med Chem*, 2017, **127**, 972-985.
17. J. Liu, C.-J. Li, L. Ni, J.-Z. Yang, L. Li, C.-x. Zang, X.-Q. Bao, D. Zhang and D.-M. Zhang, *RSC Advances*, 2015, **5**, 80553-80560.
18. N. Kaila, K. Janz, S. DeBernardo, P. W. Bedard, R. T. Camphausen, S. Tam, D. H. Tsao, J. C. Keith, Jr., C. Nickerson-Nutter, A. Shilling, R. Young-Sciame and Q. Wang, *J Med Chem*, 2007, **50**, 21-39.
19. K. He, H. Nukada, T. Urakami and M. P. Murphy, *Biochem. Pharmacol.*, 2003, **65**, 67-74.
20. V. Oliveri and G. Vecchio, *Eur J Med Chem*, 2016, **120**, 252-274.
21. R. K. Dhungana, V. Aryal, D. Niroula, R. R. Sapkota, M. G. Lakomy and R. Giri, *Angew Chem Int Ed Engl*, 2021, **60**, 19092-19096.
22. S. H. Back, J. H. Park, C. Cui and D. J. Ahn, *Nat Commun*, 2016, **7**, 10234.
23. V. K. Gupta, A. Mittal and V. Gajbe, *J. Colloid Interf. Sci.*, 2005, **284**, 89-98.
24. X. Ji, H. Huang, Y. Li, H. Chen and H. Jiang, *Angew. Chem. Int. Ed.*, 2012, **51**, 7292-7296.
25. J. A. P. Maitland, J. A. Leitch, K. Yamazaki, K. E. Christensen, D. J. Cassar, T. A. Hamlin and D. J. Dixon, *Angew Chem Int Ed Engl*, 2021, **60**, 24116-24123.
26. M. Kaur, S. Pramanik, M. Kumar and V. Bhalla, *ACS Catal.*, 2017, **7**, 2007-2021.
27. V. M. Muzalevskiy, K. V. Belyaeva, B. A. Trofimov and V. G. Nenajdenko, *J Org Chem*, 2020, **85**, 9993-10006.
28. J. Zeng, K. M. Liu and X. F. Duan, *Org Lett*, 2013, **15**, 5342-5345.
29. M. Wasa, B. T. Worrell and J. Q. Yu, *Angew Chem Int Ed Engl*, 2010, **49**, 1275-1277.
30. A. J. Johnston, K. B. Ling, D. Sale, N. Lebrasseur and I. Larrosa, *Org Lett*, 2016, **18**, 6094-6097.
31. P. Xu, P. Y. Chen and H. C. Xu, *Angew Chem Int Ed Engl*, 2020, **59**, 14275-14280.
32. A. Ramaraju, N. K. Chouhan, O. Ravi, B. Sridhar and S. R. Bathula, *European Journal of Organic Chemistry*, 2018, **2018**, 2963-2971.
33. M. Yan, J. C. Lo, J. T. Edwards and P. S. Baran, *J. Am. Chem. Soc.*, 2016, **138**, 12692-12714.
34. C. H. Schiesser, U. Wille, H. Matsubara and I. Ryu, *Acc. Chem. Res.*, 2007, **40**, 303-313.
35. M. P. Sibi and N. A. Porter, *Acc. Chem. Res.*, 1998, **32**, 163-171.
36. C. De Dobbeleer, J. Pospisil, F. De Vleeschouwer, F. De Proft and I. E. Marko, *Chem. Commun. (Camb)*, 2009, DOI: 10.1039/b901943j, 2142-2144.
37. B. Schweitzer-Chaput, M. A. Horwitz, E. de Pedro Beato and P. Melchiorre, *Nat. Chem.*, 2019, **11**, 129-135.
38. B. Giese, *Pergamon Press: Oxford. U.K.*, 1986.
39. P. R. M. Sibi, *Wiley-VCH: Weinheim, Germany*, 2001, 2001, DOI: 10.1002/9783527618293.ch8.
40. R. G. Parr, L. v. Szentpály and S. Liu, *J. Am. Chem. Soc.*, 1999, **121**, 1922-1924.
41. P. Jaramillo, P. Perez, R. Contreras, W. Tiznado and P. Fuentealba, *J. Phys. Chem. A*, 2006, **110**, 8181-8187.
42. M. W. Wong, A. Pross and L. Radom, *J. Am. Chem. Soc.*, 1993, **115**, 11050-11051.
43. P. Perez, A. Toro-Labbe, A. Aizman and R. Contreras, *J. Org. Chem.*, 2002, **67**, 4747-4752.
44. L. R. Domingo and P. Perez, *Org. Biomol. Chem.*, 2013, **11**, 4350-4358.
45. J. Liu, Y. Ye, J. L. Sessler and H. Gong, *Acc. Chem. Res.*, 2020, **53**, 1833-1845.
46. J. D. Cuthbertson and D. W. MacMillan, *Nature*, 2015, **519**, 74-77.
47. J. Dong, Z. Wang, X. Wang, H. Song, Y. Liu and Q. Wang, *Sci. Adv.*, 2019, **5**, eaax9955.
48. D. M. Schultz and T. P. Yoon, *Science*, 2014, **343**, 1239176.
49. J. H. Kim, T. Constantin, M. Simonetti, J. Lloveria, N. S. Sheikh and D. Leonori, *Nature*, 2021, **595**, 677-683.

50. T. Constantin, M. Zanini, A. Regni, N. S. Sheikh, F. Julia and D. Leonori, *Science*, 2020, **367**, 1021-1026.
51. P. Xiong, H. H. Xu and H. C. Xu, *J. Am. Chem. Soc.*, 2017, **139**, 2956-2959.
52. A. K. Sahoo, A. Dahiya, B. Das, A. Behera and B. K. Patel, *J. Org. Chem.*, 2021, **86**, 11968-11986.
53. J.-B. Xia, C. Zhu and C. Chen, *J. Am. Chem. Soc.*, 2013, **135**, 17494-17500.
54. C. Le, T. Q. Chen, T. Liang, P. Zhang and D. W. C. MacMillan, *Science*, 2018, **360**, 1010-1014.
55. J. H. Kim, A. Ruffoni, Y. S. S. Al - Faiyz, N. S. Sheikh and D. Leonori, *Angew. Chem. Int. Ed.*, 2020, **132**, 8302-8308.
56. T. Li, K. Liang, Y. Zhang, D. Hu, Z. Ma and C. Xia, *Org. Lett.*, 2020, **22**, 2386-2390.
57. J.-M. Li, Y.-H. Wang, Y. Yu, R.-B. Wu, J. Weng and G. Lu, *ACS Catal.*, 2017, **7**, 2661-2667.
58. R. A. Rossi, R. A. Alonso and S. M. Palacios, *J. Org. Chem.*, 1981, **46**, 2498-2502.
59. J. Aleman, E. Reyes, B. Richter, J. Overgaard and K. A. Jorgensen, *Chem. Commun. (Camb)*, 2007, DOI: 10.1039/b710393j, 3921-3923.
60. J. J. S. García, A. D. Hernández-Suzan, E. Martínez-Klimova, M. Flores-Alamo, T. R. Apan and E. I. Klimova, *Inter. J. Org. Chem.*, 2017, **07**, 57-81.
61. W.-D. Rudolf and R. Schwarz, *Synlett*, 1993, **1993**, 369-374.
62. W. Yu, X. Zhang, B. Qin, Q. Wang, X. Ren and X. He, *Green Chem.*, 2018, **20**, 2449-2454.
63. J. A. Leitch, A. L. Fuentes de Arriba, J. Tan, O. Hoff, C. M. Martinez and D. J. Dixon, *Chem Sci*, 2018, **9**, 6653-6658.
64. J. Hartwig, Y. Nakao, K. Semba, D. Small, A. Ohgi and N. Saper, *Chem. Rev.*, 2019, DOI: 10.26434/chemrxiv.7825844.v3.
65. L. C. Yang, Y. N. Wang, R. Liu, Y. Luo, X. Q. Ng, B. Yang, Z. Q. Rong, Y. Lan, Z. Shao and Y. Zhao, *Nat. Chem.*, 2020, **12**, 860-868.
66. Y. Moon, B. Park, I. Kim, G. Kang, S. Shin, D. Kang, M. H. Baik and S. Hong, *Nat. Commun.*, 2019, **10**, 4117.